A PRESSURIZED GAS DETECTOR FOR HIGH-ENERGY NEUTRINOS

V.K. Chernyatin[1], B.A. Dolgoshein[1], I.A. Golutvin[2], V.S. Kaftanov[3], A.N. Kalinovskii[1], V.D. Khovansky[3], V.P. Sarantsev[2], V.G. Shevchenko[3], V.V. Sosnovtsev[1], V.A. Sviridov[2] and A.V. Vishnevskii[2]

ABSTRACT

A new gas detector for high-energy neutrino physics is proposed. The working gas is an argon-xenon-propane mixture compressed to 150-200 atm. Experiments made with a small model demonstrate that in this range of pressures the proposed detector can operate in a drift-proportional mode with a space-coordinate accuracy comparable to that of large bubble chambers. A precise measurement of dE/dx is also possible.

1. INTRODUCTION

The modern electronic neutrino detectors usually combine calorimeters with magnetized iron spectrometers. The calorimeter measures a hadron energy flow. Only muons can be traced in space as separate tracks, and their momentum is measured in magnetized iron.

We propose an electronic neutrino detector of a new type, where tracks are reconstructed for all charged particles*). It represents a homogeneous detector with argon compressed up to a pressure of 120-200 atm ($\rho \simeq 0.2$-0.4 g/cm^3). Track points are measured with an accuracy comparable to that of large bubble chambers, and a precise measurement of dE/dx is also possible. At the moment no other detectors have such possibilities.

A total target mass of $\sim$ 100 tons seems to be feasible. A large target mass plus a high level of information about each event permits us to study neutrino reactions with cross-sections down to (10^{-5}-10^{-3}) σ_{tot} in the beams of even present-day accelerators.

2. WHY PRESSURIZED GAS?

The homogeneous high-pressure gas detector has a number of advantages which offer new possibilities for neutrino experiments: the mechanism of electron amplification in gas makes it easy to reach a space resolution of track coordinates that is better than 1 mm without there being any essentially new electronic developments. Since the working medium is also a neutrino target, it provides a high visibility of every event.

Compared to other detectors, the gas detector offers an excellent possibility for ionization measurements. This becomes important, for instance, in the separation of neutrino interactions with electrons from interactions with nuclei. Recoils with energy down to 1 MeV can easily be detected. The separation conditions are considerably worse for detectors based on condensed media. Even in liquid argon it is worse, because of the effects of high recombination and the absence of electron amplification.

---

1) Moscow Institute of Engineering Physics.
2) JINR, Dubna.
3) ITEP, Moscow.

*) For details, refer to preprint ITEP-53/79 (1979).

The high spatial resolution and the detailed coordinate information combined with ionization measurements make the pressurized gas detector much more informative than other neutrino detectors proposed at present.

3. THE MAIN PRINCIPLES OF THE DETECTOR

Argon is the most suitable gas for the detector (under normal conditions the density is 1.8×10^{-3} g/cm^3). Xenon and krypton are expensive, and the density of neon and helium is too low.

The geometry of the proposed detector can be seen clearly in Fig. 1. The body of the gas vessel is a stainless-steel cylinder of 2 m inner diameter embedded in an iron yoke of the superconducting magnet with H = 2 T. The mass of the argon in this vessel at 200 atm is $\sim$ 1.2 t/m; therefore to reach a mass of 100 tons the detector length should be 80 m. For the present-day accelerators the optimal size of a 100-ton detector seems to be: diameter $\sim$ 3.5 m, length $\sim$ 35 m, and pressure $\sim$ 150 atm.

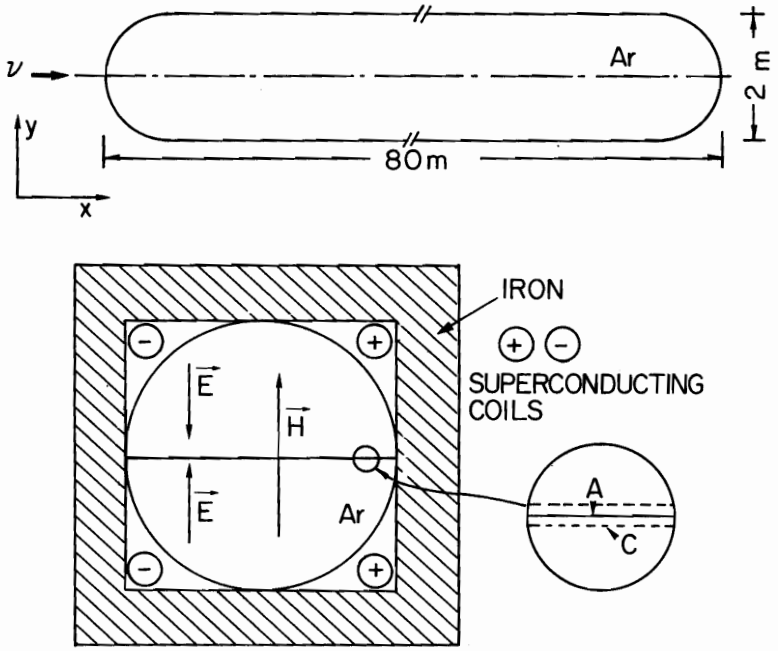

Fig. 1 The schematic view of the proposed detector: diameter 2 m, length 80 m, pressure 200 atm.

The coordinate read-out system is designed on the principle of a multiwire drift chamber, with a drift gap of $\sim$ 1 m. Such arrangements are in the process of being built [ISIS[1], TPC[2], ASTRON[3]]. In these systems the electronic image of the event, produced in gas, drifts to the multiwire anode ($\sim$ 100 wires/m), where electron amplification takes place.

We have chosen a combination of a single anode plane with two cathode planes on either side, stretched in the median plane of the cylinder (see Fig. 1). A set of wires along the surface of the cylinder forms a uniform drift field. The gap between the cathode and the anode planes is $\sim$ 10 mm; the distance (step) between the anode wires is 1-2 mm. In this geometry the magnetic and the electric fields are parallel.

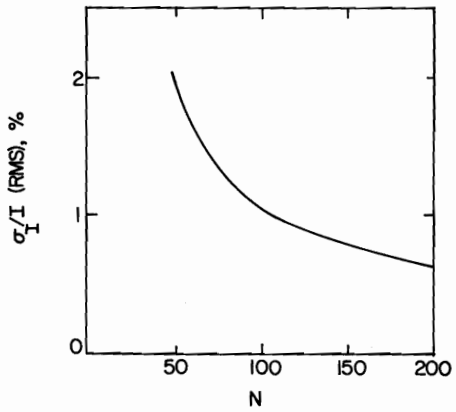

Fig. 2 Accuracy of ionization measurement as a function of the number of measurements on a 1 m track (argon, pressure 100 atm). 50% of the points with maximum ionization were rejected in the calculations (to discriminate δ-electron contribution). The remaining points were averaged.

The proposed detector as well as those mentioned above[1-3] allow precise measurements of particle ionization. As shown in Ref. 2, the accuracy of relative ionization measurement on 1 m tracks in 200 points at an argon pressure of 10 atm is $\sim$ 2% (r.m.s.). Increasing the pressure up to 100-200 atm improves the accuracy to better than 1% (see Fig. 2).

The measurement of dE/dx with an accuracy of $\sim$ 1% in the region of the relativistic rise of ionization losses ($\eta = p/m \leq 50$) allows identification of particle masses with known momentum.

The coordinate z along the drift field is determined by the drift time: $z = v_d \times t_d$, where v_d is the drift velocity and t_d is the drift time. The coordinate across the drift field is measured as in the multiwire proportional chamber (i.e. anode wire number + cathode read-out).

The following questions are of great importance:

i) Electron amplification in a gas at a pressure of 100-200 atm.

ii) Drift velocity and its dependence on the drift field.

iii) Diffusion of drifting electrons.

iv) Ionization measurements.

v) An electron attachment during the drift which affects the accuracy of ionization measurements.

vi) Space-charge effects of positive ions in the drift gap.

4. EXPERIMENTAL STUDY ON A SMALL MODEL

Detailed studies of a cylindrical proportional counter[4] filled with pressurized argon, as well as with mixtures of argon with methane and xenon, show that electron amplification of $\sim 10^4$ can be reached at a pressure of up to 100 atm. However, data on electron drift velocities and diffusion processes are not yet known for these conditions. We studied them

with a small model of a multiwire drift chamber filled with different gas mixtures. The drift chamber used is shown schematically in Fig. 3. The drift gap is 35 mm; the anode plane is of gold-plated tungsten wires, 20 μm in diameter, spaced by 2 mm. The gap between the cathode and the anode planes is 4.5 mm.

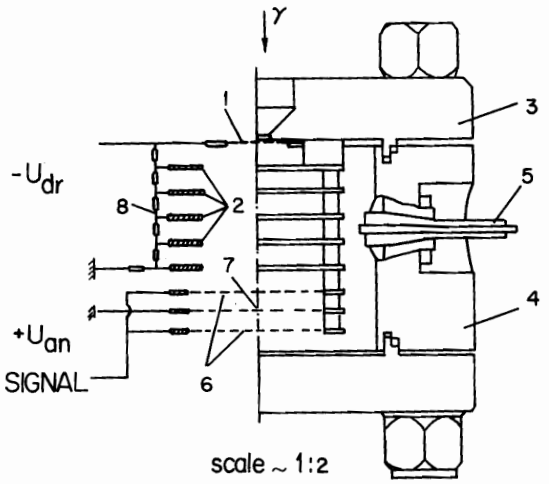

1) Upper "drift grid"
2) Metal rings equalizing the electric field in the drift space
3) Upper flange with aluminium window, 0.4 mm thick.
4) High-pressure frame
5) High-voltage input
6) Cathode grid
7) Anode grid
8) Drift voltage divider

Fig. 3 Schematic view of the drift chamber model

4.1 Drift velocity

To measure the drift velocity, electrons were produced in the chamber gas by means of a pulsed X-ray tube. The drift time of the electrons, produced near the drift grid and moving to the cathode plane, was measured by the duration of the cathode current pulse. The results of the measurements are presented in Fig. 4.

Comparing these data with others obtained at low pressures, we can conclude that the drift velocities at 150 atm and at 1 atm are the same within 3% if E/p is kept constant.

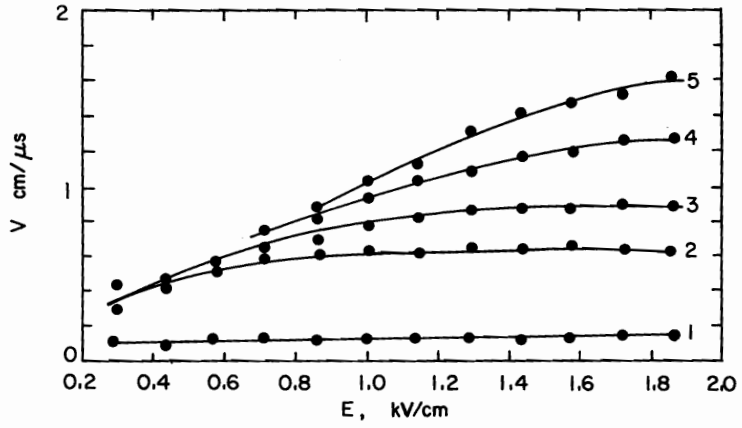

Fig. 4 Electron drift velocity as a function of the electric field at a pressure of 100 atm: 1) Ar + 0.5% Xe; 2) Ar + 0.5% Xe + 0.1% CH_4; 3) Ar + 0.5% Xe + 0.2% CH_4; 4) Ar + 0.5% Xe + 0.5% CH_4; 5) Ar + 0.5% Xe + 1.0% CH_4.

4.2 Gas amplification

To measure the gas amplification, the chamber was exposed to γ-rays of a ^{241}Am source (E_{γ_1} = 26.4 keV, E_{γ_2} = 59.6 keV). The results of the measurements are shown in Fig. 5. The addition of up to 2% of methane, as shown in Fig. 5, shifts the amplitude characteristics to the right.

The effect of adding xenon to the gas was studied with a methane content of 0.1% and 0.2%. The admixture of xenon and argon at high pressure, as mentioned in Ref. 4, reduces the anode voltage considerably (see Fig. 6). The dependence of the anode voltage at k = 10^2 and 10^3 on the pressure of the Ar + 0.5% Xe + 0.2 CH_4 mixture is illustrated in Fig. 7.

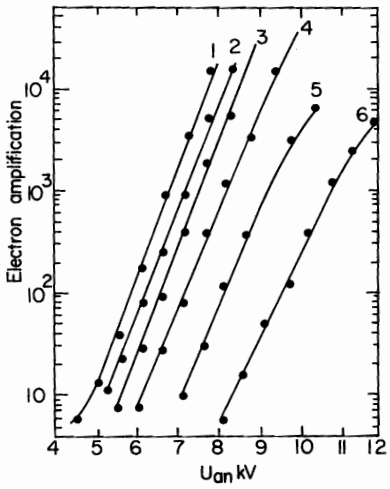

Fig. 5 Electron amplification as a function of V_{an} (Pressure: 100 atm). 1) Ar + 0.5% Xe; 2) Ar + 0,5% Xe + 0.1% CH_4; 3) Ar + 0.5% Xe + + 0.2% CH_4; 4) Ar + 0.5% Xe + 0.5% CH_4; 5) Ar + 0.5% Xe + 1.0% CH_4; 6) Ar + 0.5% Xe + + 2.0% CH_4.

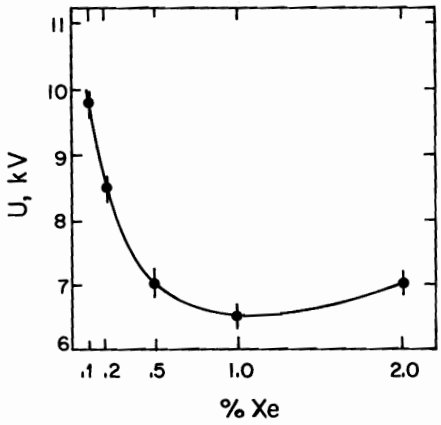

Fig. 6 Anode voltage as a function of xenon concentration for an electron amplification of 10^3 in Ar + 0.2% CH_4 + Xe mixture. (Pressure: 100 atm.)

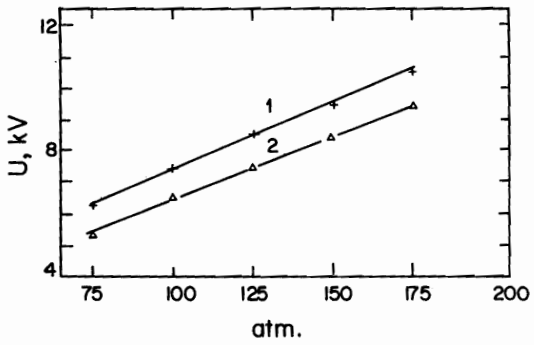

Fig. 7 Anode voltage as a function of pressure for an electron amplification of 10^3 (1) and 10^2 (2). Gas mixture: Ar + + 0.5% Xe + 0.2% CH_4.

4.3 Electron diffusion

In order to measure the electron diffusion, the chamber was exposed to γ-rays with an energy of ≤ 13 keV from an X-ray tube. The electron drift distance from the point of γ-absorption to the anode plane was ∿ 4 cm. The cloud width was measured from a current pulse width, and it was found to be ∿ 780 μm (FWHM) (Ar + 0.5% Xe, 100 atm, drift field 1 kV/cm). This corresponds to a standard deviation of electron diffusion $\sigma = (160 \pm 10)\sqrt{z}$ μm·cm$^{-1/2}$,

where z is the drift distance; σ, evaluated from the value of the longitudinal diffusion coefficient D_L [5] for the case of normal pressure, is

$$\sigma = \sqrt{\frac{2 \cdot D_L \cdot z}{P \cdot v_d}} \simeq 140\sqrt{z}\ \mu m \cdot cm^{-1/2} .$$

It can be seen that diffusion at P = 150 atm on a drift path of z = 150 cm is the same as for P = 1 atm and z = 1 cm. So, for the proposed detector the inaccuracy due to diffusion is not more than 100-150 μm.

4.4 Electron attachment and space-charge effects

We did not study these questions experimentally. To get 1% precision in ionization measurements on a drift path of 1 m, the contamination of electronegative gases (mainly oxygen) should be less than 10^{-2} ppm. Studies made elsewhere[2,6] have demonstrated that this purity can be achieved.

Another problem is that of a space charge of positive ions produced in an avalanche near the anode wires. Their field affects the gas amplification factor as well as creating the inhomogeneity of the drift field itself. If we use the results of Friderich et al.[7], where these effects were thoroughly studied, we conclude that space-charge effects are negligible for an electron amplification of 10^2-10^3 (assuming that in neutrino experiments the main source of background is cosmic rays).

5. COMPUTER SIMULATION

To find out what a real neutrino event will look like in a pressurized gas detector, we simulated neutrino events (recorded in the bubble chamber SKAT) in the neutrino beam of the IHEP. For these calculations we assumed that the accuracy of track reconstruction along and across the drift field is $\sigma_z = \sigma_x = 200$ μm. Figure 8a shows the result of a simulation of an event $\nu_\mu + N \to \mu^- + e^+ + \pi + 3p$. In Fig. 8b the magnified part of the vertex region is shown. From this figure it is clear that in a multiprong event, tracks can be measured down to ∿ 5 mm from the vertex. A two-track resolution is of ∿ 2 mm.

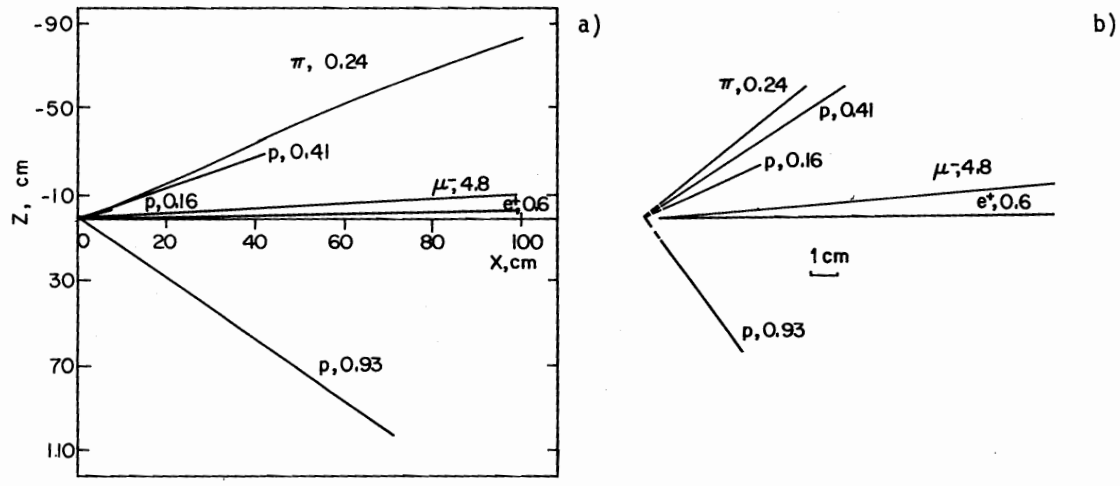

Fig. 8 a) An example of the simulation, in the gas detector, of a real neutrino event $\nu_\mu + N \to \mu^- + e^+ + \pi + 3p$ detected in the bubble chamber SKAT. Only the first 100 cm of each track are shown. The symbols above the tracks indicate the type of particle and its momentum in GeV/c. (Pressure: 100 atm.) b) A more detailed view of the event near the vertex. Dashed lines indicate those parts of the tracks which are not resolved in space. The simulation was done without a magnetic field.

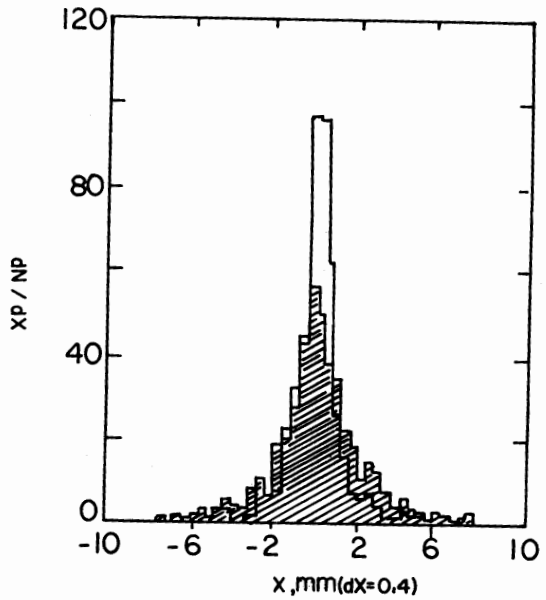

Fig. 9 The distribution of the vertices along the neutrino beam. Black histogram: without multiple scattering. Shaded histogram: with multiple scattering. (Pressure: 100 atm.)

In Fig. 9 one can find the distribution of the deviation of the calculated vertex from the true one in the direction of the beam. The width was found to be σ_{ver} = 1.2 mm, which is comparable to the accuracy for large bubble chambers.

The results of the simulation also proved that the angular resolution is defined mainly by multiple scattering in gas and is equal to $\sigma_\theta \leq 3$ mrad for $p \geq 3$ GeV/c.

6. SUMMARY OF DETECTOR CHARACTERISTICS

i) The total mass of gas is 100 tons.
Two solutions are possible:
a) diameter 2 m, length 80 m, pressure 200 atm; or
b) diameter 3.5 m, length 35 m, pressure 150 atm.
The nuclear interaction length at 150 atm is $\sim$ 3.3 m; the radiation length $\sim$ 73 cm.

ii) The magnetic field is $\sim$ 2 T.

iii) The gas mixture is Ar + 0.5% Xe + (0.1-0.5)% CH_4.
The electron drift velocity is (5-10) $\times$ 10^5 cm/s for drift fields of 1-2 kV/cm. A maximum drift time is 100-200 μs.

iv) The space resolution $\sigma \simeq 200$ μm in all directions.

v) dE/dx can be measured with an accuracy of $\sim$ 1%.

7. CONCLUSIONS

The experiments made with a small model, together with data from other studies, have shown that the proposed new detector with pressurized argon can have a high spatial resolution and precise ionization measurements. It can be used to study neutrino interactions on

a new level of information about each event. It has obvious advantages for investigating pure leptonic reactions.

The measurement of ionization on a track path of 5-10 mm provides the unique chance to distinguish clearly the νN interactions on a nucleus from νe interactions. Heavy ionizing recoils are easily detected. This is particularly important for the study of rare processes (νe scattering, trident production, τ physics) with cross-sections of 10^{-5}-10^{-3} of σ_{tot}.

REFERENCES

1) W.W.M. Allison et al., Nucl. Instrum. Methods 19, 499 (1974).

2) A.R. Clark et al., Proposal for PEP facility based on the time projection chamber, PEP-4, December 30, 1976.

3) A.I. Babaev et al., Preprint ITEP-103 (1978).

4) V.Kh. Dodokhov et al., Dubna JINR P13-11869 (1978).

5) I.H. Parker et al., Phys. Rev. 181, 290 (1969).

6) Z.P. Uteshev, Thesis, Moscow Institute of Engineering Physics (1979).

7) D. Friderich et al., Nucl. Instrum. Methods 158, 81 (1979).